Eur. Phys. J. D **24**, 27–32 (2003)
DOI: 10.1140/epjd/e2003-00176-7

THE EUROPEAN PHYSICAL JOURNAL D

Theoretical determination of electron binding energy spectra of anionic magnesium clusters

P.H. Acioli[a] and J. Jellinek[b]

Chemistry Division, Argonne National Laboratory, Argonne, Illinois 60439, USA

Received 10 September 2002
Published online 3 July 2003 –

Abstract. A recently developed accurate scheme for converting the single-particle eigenenergies of the density functional theory into electron binding energies is used to compute the spectra of electron binding energies in Mg_4^-, Mg_{11}^-, Mg_{16}^-, and Mg_{18}^-. The computations are performed for different isomeric forms of the clusters using both pseudopotential and all-electron treatments. The results are compared with the data derived from electron photodetachment experiments, and the role of the different isomers in the interpretation of these data is examined.

PACS. 36.40.-c Atomic and molecular clusters – 33.60.-q Photoelectron spectra – 31.15.Ew Density-functional theory – 33.15.Ry Ionization potentials, electron affinities, molecular core binding energy

1 Introduction

Electronic spectroscopy is a powerful tool in studies of structural and electronic properties of finite systems, be they atoms, molecules, or clusters [1]. As applied to clusters [2], electronic spectroscopy can shed light on how their properties change with cluster size. The size-dependence of cluster features is one of the most, if not the most, fascinating attributes of these systems, and metal clusters form an especially interesting (and challenging, one might add) area of the cluster field [3–5]. An illustration of this is the fact that small atomic clusters of elements, which are metals in bulk quantities, may not possess metallic characteristics, or even properties that could be viewed as the precursor, or finite-size analog, of these characteristics ([6–10]; and references therein). The emergence of metal-like properties and their evolution into true metallic attributes, as a cluster grows in size, is reflected in and can be characterized by the evolution of its electronic features. These latter are, of course, coupled with the structural characteristics. Electronic spectroscopy can thus be used to interrogate the size-induced nonmetal-to-metal transition. Its utility, however, is much broader, since electronic states and their densities are among the most fundamental properties of systems, and their knowledge allows for characterization of other features.

On the theoretical/computational side, density functional theory (DFT) is the approach of choice in electronic structure computations on medium and large size systems. For metals this is true even for smaller clusters in view of the usually considerable (especially for transition metals) number of electrons to be treated, and the necessity to consider different possible isomeric forms of the clusters. An inherent limitation of the Kohn-Sham (KS) single-particle form of DFT is that its eigenenergies correspond to auxiliary quasiparticles, rather than real electrons. Therefore these (KS) eigenenergies have to be corrected to make them eigenenergies (or, equivalently, negative of binding energies) of electrons. A variety of correction schemes was considered in the past. They either are limited to particular implementations of DFT (*e.g.*, the local density approximation), have limited accuracy, or lack rigorous justification (a brief review is given in Ref. [11]). Recently, we have formulated a new general scheme for computation of the needed corrections [11] and applied it to study the phenomenon of size-induced nonmetal-to-metal transition in Mg clusters [7,8]. This transition has been the subject of two new experimental studies [9,10].

Here we present results of the application of the new scheme in computations of the spectra of electron binding energies for Mg_4^-, Mg_{11}^-, Mg_{16}^- and Mg_{18}^- clusters. These four are selected as their measured spectra [10] represent different characteristic patterns. A sketch of the methodology is given in the next Section. The results are presented and analyzed in Section 3. A brief summary is given in Section 4.

[a] *Permanent address:* Núcleo de Física Atômica, Molecular e Fluidos, Instituto de Física, Universidade de Brasília, CP 04455, Brasília, DF, 70919-970, Brazil.
[b] e-mail: jellinek@anl.gov

2 Methodology

The computations are performed using the gradient-corrected version of DFT with the Becke exchange [12] and Perdew′86 [13] correlation functionals (BP′86). The two $3s$ electrons of each magnesium atom plus the extra electron of the cluster anion (the "valence electrons") are treated explicitly using a contracted Gaussian basis set of the type (21|21), which is used in combination with the Wadt-Hay [14] pseudopotential representation of the ionic cores of the atoms. This selection of the exchange-correlation functional and the pseudopotential/basis set is based on tests performed on neutral Mg_n, $n = 1-5$, clusters (for details see Ref. [8]), and it was used in our earlier studies [7,8]. Predicated on the tests, we expect good agreement between the results of the pseudopotential and all-electron computations. To verify this expectation we repeated all the computations with the 6-31G* all-electron basis set [15]. Results of earlier theoretical studies of primarily neutral magnesium clusters using alternative quantum chemical and density functional approaches can be found in references [16–28].

The search for the isomeric forms of the anionic clusters was performed using gradient-based techniques with no symmetry constraints imposed. A variety of configurations, both symmetric and asymmetric, was used as initial guess structures for each cluster size. Normal mode analysis was applied to each stationary configuration obtained, and only those with all positive frequencies qualified as isomers.

The computations of the structures also provide the spectra of their KS eigenenergies. As mentioned, we have used our new correction scheme to convert these eigenenergies into spectra of the corresponding electron binding energies. The details are presented elsewhere [7,8,11]. Here we mention only that the new scheme is based on the following conceptual considerations. The vertical binding (detachment) energy of the most external electron of an N-electron system can be computed for any fixed geometrical structure of the system as the difference between the ground state total electronic energies of this structure with $N-1$ and N electrons, respectively. These total energies are defined within any version of DFT rigorously. The additive "HOMO" correction needed to obtain the binding energy of the most external electron in this structure from the negative of its KS HOMO eigenenergy is then by definition the difference between the latter two.

Keeping the structure of the system fixed and removing sequentially the least bound electron, one can convert any electron of the system into the most external one. The HOMO correction to the KS eigenenergy of an arbitrary electron, when it is the most external, can be computed as defined above. The thus obtained set of the structure- and orbital-specific HOMO corrections is then evolved *via* an interpolation procedure to give the corrections to the individual KS eigenenergies as they shift with the restoration ("putting back") of the electrons in the system. The outcome of the procedure is the additive corrections that convert the negative of the different KS eigenenergies of the N-electron system into the binding energies of the corresponding electrons.

The merits of the new correction scheme are: (1) it is applicable to any implementation of DFT; (2) it uses only quantities rigorously defined within DFT; (3) it yields orbital- or, alternatively, electron-specific corrections; (4) it furnishes highly accurate electron binding energies, provided these energies are reproduced by the chosen version of DFT accurately when the electrons play the role of the most external one (results of tests on atoms of ten elements and three molecules are given in Ref. [11]). All-electron BP′86 computations with the 6-31G* basis set on the Mg atom yield electron binding energies that are on average within 1.3% of the measured values. As mentioned, the corrections to the KS eigenenergies are structure-specific. In what follows we consider the anionic magnesium clusters fixed in their respective isomeric forms.

3 Results

In earlier studies [7,8], which focused on the size-induced nonmetal-to-metal transition, we have shown that the size-dependence of the difference in the computed binding energies of the two most external electrons of Mg_n^-, $n = 2-22$, clusters, each considered in its most stable structure, is in good agreement with the data derived from the experiments [10]. This difference is the anionic finite-size analog of the gap between the valence and the conduction bands in the bulk (*cf.* the discussion in Refs. [7,8]), and therefore it can serve as an indicator of the degree of metallicity. Here we consider four clusters, Mg_4^-, Mg_{11}^-, Mg_{16}^-, and Mg_{18}^-, for which the computed difference in the mentioned binding energies is 1.493 eV, 0.461 eV, 0.245 eV, and 0 eV, respectively. But, instead of the difference, here we focus on the electron binding energies themselves, and not only for the two most external electrons. In addition, for each cluster we consider not only its most stable configuration, but all the isomers identified for it. The structural and energy characteristics of the isomers are summarized in Table 1. For each cluster size, the energies are referred to that of the most stable configuration.

The only stable equilibrium structure we found for Mg_4^- is a tetrahedron (see Fig. 1) with a bond length of 3.076 Å or 3.086 Å as obtained within the pseudopotential and the all-electron computations, respectively. For Mg_{11}^- we have identified two isomers (see Fig. 2) with very close energies. The structure of the second isomer with C_{2v} symmetry is only slightly distorted from that of a perfect D_{3h} pentacapped trigonal prism. The search produced three isomers for Mg_{16}^- (see Fig. 3). The first two, both of C_s symmetry, have close energies, while the third has a higher energy. The C_{3v} symmetry of the third isomer, as obtained within the pseudopotential computation, gets reduced to the C_s symmetry of the close but slightly distorted form of this isomer furnished by the all-electron treatment. Three isomers were also found for Mg_{18}^- (see Fig. 4). Whereas all

Table 1. Isomeric forms (Iso), their symmetries (Sym) and configurational energies (ΔE) of the four clusters. For each cluster the energies are referred to that of its most stable structure. The isomers obtained within the pseudopotential and the all-electron approaches are labeled by roman and arabic numerals, respectively.

Cluster	Pseudopotential			All-electron		
	Iso	Sym	ΔE(eV)	Iso	Sym	ΔE(eV)
Mg_4^-	I	T_d	0	1	T_d	0
Mg_{11}^-	I	C_s	0	1	C_s	0
	II	C_{2v}	0.043	2	C_{2v}	0.061
Mg_{16}^-	I	C_s	0	1	C_s	0
	II	C_s	0.098	2	C_s	0.056
	III	C_{3v}	0.377	3	C_s	0.216
Mg_{18}^-	I	C_{4v}	0	1	C_{2v}	0
	II	C_{2v}	0.008	2	C_{4v}	0.024
	III	C_s	0.025	3	C_s	0.034

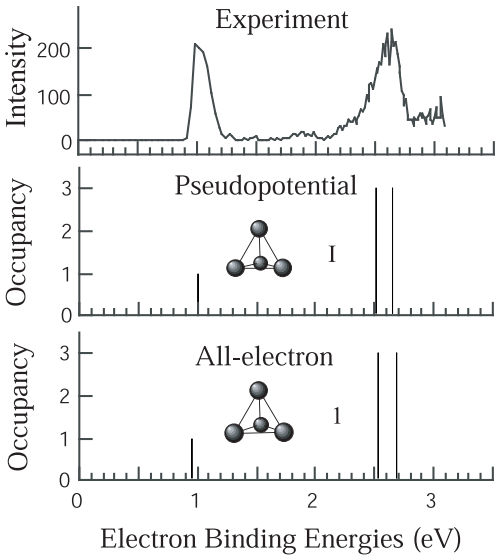

Fig. 1. The measured [10] and computed electron binding energies of the single isomer of Mg_4^-.

three are almost degenerate within both the pseudopotential and the all-electron computations, the two treatments invert the energy ordering of the first two isomers. Also, the second isomer emerges as energetically closer to the first one in the pseudopotential treatment and to the third one in the all-electron computation. Overall, the two treatments give very similar results. As a final remark on the structural forms we mention that, with the exception of the C_{4v} isomer of Mg_{18}^-, they all correspond to the doublet spin-multiplicity state. The spin state of the C_{4v} isomer is a quartet.

In Table 2 we list the KS eigenenergies, the corresponding corrections, and the obtained from these binding energies of the valence electrons of the Mg_4^- cluster (note that the KS HOMO eigenenergy is positive in this case, but this poses no problem in the new correction scheme [7,8,11]). The computed binding energies with values less than or

Table 2. The KS eigenenergies (ε) of the valence orbitals of the Mg_4^- cluster, and the corresponding corrections (Δ) and electron binding energies (BE), all in units of eV. α and β label the majority and the minority spins, respectively. The numbers in brackets indicate the number of electrons (occupancy) in the different orbitals.

Orbital	Pseudopotential			All-electron		
	$-\varepsilon$	Δ	BE	$-\varepsilon$	Δ	BE
$a_1(\alpha)[1]$	–0.603	1.614	1.012	–0.663	1.608	0.945
$t_2(\beta)[3]$	0.841	1.664	2.505	0.877	1.661	2.538
$t_2(\alpha)[3]$	0.984	1.670	2.654	1.012	1.666	2.678
$a_1(\beta)[1]$	3.612	1.816	5.428	3.465	1.804	5.269
$a_1(\alpha)[1]$	3.723	1.821	5.544	3.674	1.814	5.488

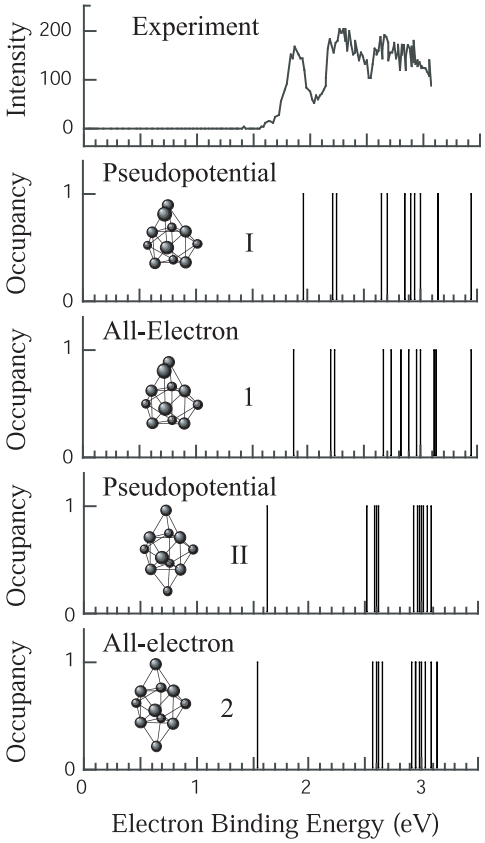

Fig. 2. The measured and computed electron binding energies of the Mg_{11}^- cluster. The numbers label the isomers as defined in Table 1.

equal to 3.5 eV are presented graphically and compared with the available measured spectrum of electron binding energies [10] in Figure 1. The results of the pseudopotential and all-electron computations are very close, and both are in excellent agreement with the measured data.

A similar comparison for the Mg_{11}^- cluster is presented in Figure 2. Again, the pseudopotential and the all-electron results are in good agreement. But only for the first isomer do the electron binding energies match all the features of the measured spectrum. The least bound electron of the second isomer appears not to be represented in the experimental data.

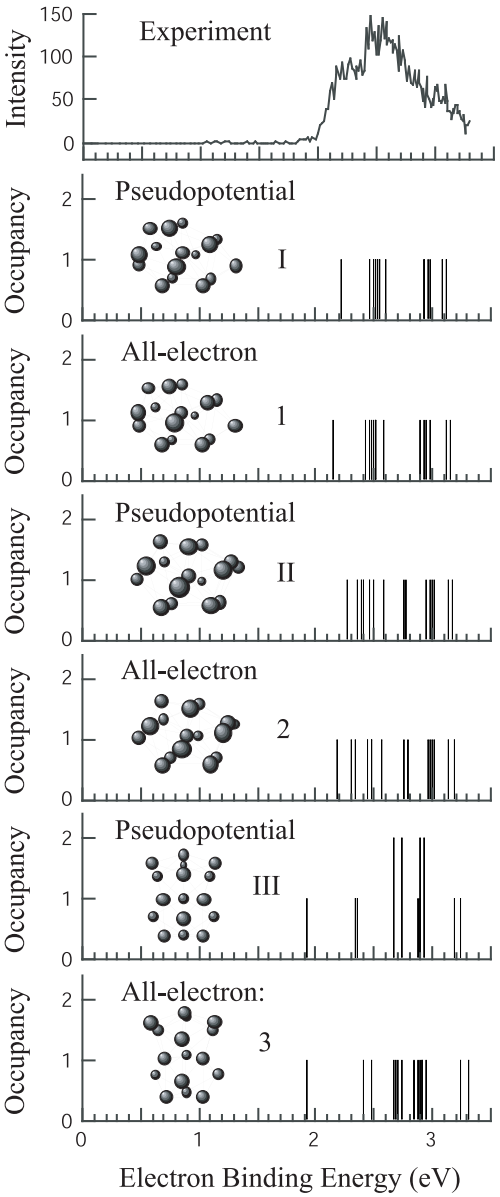

Fig. 3. The measured and computed electron binding energies of the Mg_{16}^- cluster. The numbers label the isomers as defined in Table 1.

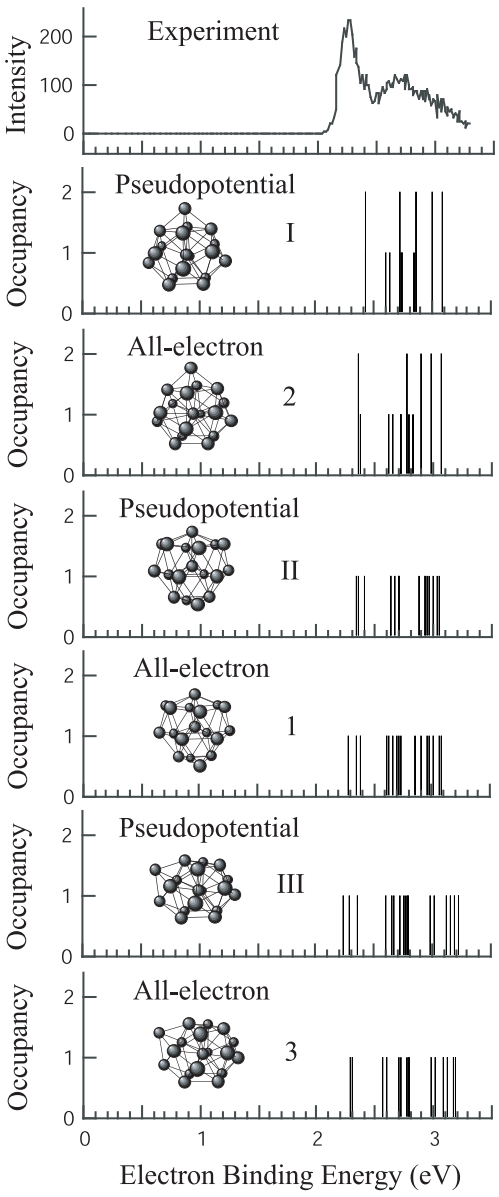

Fig. 4. The measured and computed electron binding energies of the Mg_{18}^- cluster. The numbers label the isomers as defined in Table 1.

The results for Mg_{16}^- are given in Figure 3. Whereas the overall agreement between the pseudopotential and the all-electron values is good for all three isomers, it is particularly close for the most stable structure of the cluster. And it is this structure for which the pattern of the distribution of the electron binding energies matches the shape of the experimental spectrum very well. One should note though that over the range considered, all the binding energies for the second isomer, – these are distributed more evenly than those for either the first or the third isomer, – fall under the experimental spectrum. Therefore, and taking into account that the configurational energies of the first two isomers are very close, one cannot claim with certainty that the second isomer is not represented in the measured data. Such a claim can, however, be made for the third isomer. The least bound electron of the latter has no trace in the experimental spectrum.

Data analogous to those in Table 2, but for the three isomers of Mg_{18}^-, are presented in Table 3. The pseudopotential and the all-electron approaches yield very close electron binding energies. One should notice, however, that the two treatments switch the energy ordering of the KS eigenenergies and the corresponding electron binding energies for some orbitals of the first two isomers of the cluster.

The computed results for Mg_{18}^- are displayed graphically together with the measured data in Figure 4. Inspection of the graphs shows that whereas for the C_{4v} isomer (isomer I, as defined by the pseudopotential treatment; *cf.* Tab. 1) the electron binding energies tend to bunch into

Table 3. The same as Table 2, but for the three isomers of Mg_{18}^- and KS eigenenergies whose corresponding electron binding energies are less than or equal to 4.2 eV.

Sym	Orbital	Pseudopotential			All-electron		
		$-\varepsilon$	Δ	BE	$-\varepsilon$	Δ	BE
			Iso I			Iso 2	
	$e(\alpha)[2]$	1.173	1.254	2.427	1.109	1.250	2.359
	$a_1(\alpha)[1]$	1.178	1.254	2.432	1.131	1.250	2.381
	$a_1(\beta)[1]$	1.341	1.256	2.596	1.393	1.254	2.647
	$b_2(\beta)[1]$	1.371	1.256	2.627	1.367	1.254	2.621
	$e(\beta)[2]$	1.469	1.257	2.726	1.519	1.256	2.774
	$b_2(\alpha)[1]$	1.470	1.257	2.727	1.466	1.256	2.722
C_{4v}	$b_1(\beta)[1]$	1.472	1.257	2.729	1.460	1.255	2.715
	$a_1(\alpha)[1]$	1.478	1.257	2.736	1.525	1.257	2.782
	$b_1(\alpha)[1]$	1.578	1.259	2.837	1.568	1.258	2.826
	$e(\alpha)[2]$	1.605	1.259	2.864	1.641	1.259	2.899
	$e(\beta)[2]$	1.732	1.260	2.992	1.724	1.259	2.983
	$e(\alpha)[2]$	1.815	1.262	3.076	1.813	1.260	3.073
	$a_1(\beta)[1]$	2.354	1.269	3.623	2.450	1.270	3.720
	$a_1(\alpha)[1]$	2.761	1.274	4.035	2.833	1.276	4.109
			Iso II			Iso 1	
	$b_2(\alpha)[1]$	1.109	1.237	2.347	1.050	1.240	2.290
	$a_1(\beta)[1]$	1.126	1.238	2.364	1.115	1.241	2.356
	$a_1(\alpha)[1]$	1.164	1.238	2.403	1.148	1.241	2.389
	$b_1(\beta)[1]$	1.392	1.242	2.634	1.367	1.243	2.610
	$b_2(\beta)[1]$	1.393	1.242	2.635	1.391	1.244	2.635
	$a_1(\beta)[1]$	1.433	1.243	2.676	1.472	1.244	2.716
	$a_1(\alpha)[1]$	1.453	1.243	2.696	1.494	1.247	2.742
	$b_1(\alpha)[1]$	1.454	1.243	2.697	1.423	1.244	2.668
	$b_2(\alpha)[1]$	1.457	1.243	2.700	1.452	1.245	2.697
C_{2v}	$a_2(\beta)[1]$	1.624	1.246	2.870	1.615	1.245	2.860
	$a_2(\alpha)[1]$	1.679	1.247	2.925	1.669	1.247	2.916
	$a_1(\beta)[1]$	1.686	1.247	2.933	1.707	1.246	2.953
	$b_2(\beta)[1]$	1.693	1.247	2.940	1.711	1.247	2.958
	$a_1(\alpha)[1]$	1.709	1.247	2.956	1.730	1.248	2.978
	$b_2(\alpha)[1]$	1.744	1.248	2.992	1.762	1.249	3.011
	$b_1(\beta)[1]$	1.788	1.249	3.036	1.823	1.248	3.071
	$b_1(\alpha)[1]$	1.799	1.249	3.047	1.834	1.249	3.083
	$a_1(\beta)[1]$	2.503	1.260	3.763	2.573	1.259	3.832
	$a_1(\alpha)[1]$	2.627	1.262	3.889	2.691	1.260	3.951
			Iso III			Iso 3	
	$a''(\alpha)[1]$	1.008	1.234	2.242	1.011	1.230	2.241
	$a'(\beta)[1]$	1.048	1.235	2.283	1.047	1.231	2.278
	$a''(\alpha)[1]$	1.115	1.236	2.351	1.071	1.232	2.303
	$a'(\beta)[1]$	1.354	1.240	2.594	1.324	1.236	2.560
	$a'(\alpha)[1]$	1.410	1.241	2.651	1.374	1.237	2.611
	$a''(\beta)[1]$	1.432	1.241	2.673	1.442	1.239	2.680
	$a''(\alpha)[1]$	1.482	1.242	2.724	1.473	1.239	2.712
	$a''(\beta)[1]$	1.506	1.242	2.748	1.493	1.240	2.732
	$a''(\alpha)[1]$	1.537	1.243	2.780	1.545	1.241	2.785
C_s	$a'(\beta)[1]$	1.538	1.243	2.781	1.551	1.241	2.792
	$a'(\alpha)[1]$	1.545	1.243	2.788	1.560	1.241	2.801
	$a'(\beta)[1]$	1.738	1.246	2.985	1.745	1.244	2.990
	$a'(\alpha)[1]$	1.770	1.247	3.017	1.777	1.245	3.021
	$a''(\beta)[1]$	1.870	1.248	3.118	1.847	1.246	3.093
	$a''(\alpha)[1]$	1.902	1.249	3.151	1.884	1.247	3.131
	$a'(\beta)[1]$	1.938	1.250	3.188	1.931	1.247	3.178
	$a'(\alpha)[1]$	1.969	1.250	3.219	1.956	1.248	3.204
	$a'(\beta)[1]$	2.333	1.257	3.590	2.411	1.256	3.667
	$a'(\alpha)[1]$	2.458	1.259	3.717	2.532	1.258	3.790

two manifolds (this is more pronounced in the all-electron results), these energies for the C_{2v} and C_s isomers (isomers II and III) group into three manifolds. In this respect, the electron binding energies of isomer I match the overall bimodal pattern of the measured spectrum better than those of isomers II and III. However, as evaluated over the range covered by the experiments, the measured spectrum may contain contributions from all three energetically close isomers.

The above results clearly show that the measured spectra of electron binding energies can be analyzed in terms of the computed isomer-specific electron binding energies as obtained within the DFT. Examination of the corrections Δ that convert the KS eigenenergies into electron binding energies (see Tabs. 2 and 3), as computed using the new scheme [7,8,11], shows that for a given isomer of the cluster the values of Δ depend only weakly on the orbital. This is true at least for the valence orbitals, and the dependence decreases as the cluster size increases. Moreover, the dependence of the corrections on the isomeric form of the cluster also appears to be only weak. Although these observations seem to be quite general [29], tests on a case by case basis are recommended.

As illustrated by the paradigms of Mg_{11}^- and Mg_{16}^-, comparison of the computed electron binding energies with the measured spectra may eliminate certain isomeric forms from the consideration. But the situation is not always clearcut. As discussed in the context of the analysis of the data for the Mg_{16}^- and Mg_{18}^- clusters, the experimental spectra may contain contributions from different isomers. This is especially true if the experiments are performed at elevated temperatures (the notion "elevated" is, of course, used here as a relative term). A quantitative evaluation of the temperature-dependent contribution of the individual isomers will require computation of the densities of states. An experimental verification of this evaluation will need measuring the spectra at different temperatures.

4 Summary

In this paper we presented results of computations on the electron binding energies for four anionic magnesium clusters. These are obtained within the BP′86 version of DFT combined with a new accurate correction scheme for converting the KS eigenenergies into electron binding energies. The latter are computed for different isomeric forms of the clusters using both pseudopotential-based and all-electron treatments. The two yield very similar results. For a given cluster size, the correction terms, although in general orbital-dependent, are found to depend only weakly on the KS eigenenergies, at least those that correspond to valence orbitals. They depend also only weakly on the isomeric form of the cluster.

The computed electron binding energies are compared with the available measured spectra. The shapes of the spectra for different cluster sizes are matched very well by the patterns of the binding energies corresponding to the most stable structures of the clusters. In some cases,

the comparison allows for elimination of an isomer as a contributor to the spectrum. In others, the indications are that more than one isomer may contribute to the spectrum. The study illustrates how a combined analysis of the computed and measured electron binding energies can shed light on the intricate interplay between the structural and electronic properties of systems, in general, and clusters, in particular.

We thank Prof. K. Bowen for providing us the experimental data. Work performed under the auspices of the Office of Science, Division of Chemical Science, U.S. Department of Energy under Contract number W-31-109-Eng-38. PHA was also supported by CNPq.

References

1. D.W. Turner, C. Baker, A.D. Baker, C.R. Brundle, *Molecular Photoelectron Spectroscopy: A Handbook of He 584 Å Spectra* (Wiley-Interscience, London, 1970); J. Berkowitz, *Photoabsorption, Photoionization, and Photoelectron Spectroscopy* (Academic Press, New York, 1979)
2. See, *e.g.*, L.-S. Wang, H. Wu, Z. Phys. Chem. **203**, 45 (1998) and references therein
3. *Clusters of Atoms and Molecules*, edited by H. Haberland (Springer-Verlag, Heidelberg, 1994), Vols. 1 and 2
4. *Theory of Atomic and Molecular Clusters, With a Glimpse at Experiments*, edited by J. Jellinek (Springer-Verlag, Heidelberg, 1999)
5. *Metal Clusters*, edited by W. Eckardt (Wiley, Chichester, 1999)
6. C. Brechignac, M. Broyer, P. Cahuzac, G. Delacretaz, P. Labastie, L. Wöste, Chem. Phys. Lett. **120**, 559 (1985); K. Rademann, B. Kaiser, U. Even, F. Hensel, Phys. Rev. Lett. **59**, 2319 (1987); C. Brechignac, M. Broyer, P. Cahuzac, G. Delacretaz, P. Labastie, J.P. Wolf, L. Wöste, *ibid.* **60**, 275 (1988); M.E. Garcia, G.M. Pastor, K. Bennemann, *ibid.* **67**, 1142 (1991); H. Haberland, B. von Issendorf, Y. Yufeng, T. Kolar, *ibid.* **69**, 3212 (1992); R. Busani, M. Folkers, O. Cheshnovsky, *ibid.* **81**, 3836 (1998)
7. P.H. Acioli, J. Jellinek, Phys. Rev. Lett. **89**, 213402 (2002)
8. J. Jellinek, P.H. Acioli, J. Phys. Chem. A **106**, 10919 (2002); **107**, 1670 (2003)
9. T. Diederich, T. Döppner, J. Braune, J. Tiggesbaunker, K.-H. Meiwes-Broer, Phys. Rev. Lett. **86**, 4807 (2001)
10. O.C. Thomas, W. Zheng, S. Xu, K.H. Bowen Jr, Phys. Rev. Lett. **89**, 213403 (2002)
11. J. Jellinek, P.H. Acioli, J. Chem. Phys. **118**, 7783 (2003)
12. A.D. Becke, Phys. Rev. A **38**, 3098 (1988)
13. J.B. Perdew, Phys. Rev. B **33**, 8822 (1986)
14. W.R. Wadt, P.J. Hay, J. Chem. Phys. **82**, 284 (1985)
15. M.M. Francl *et al.*, J. Chem. Phys. **77**, 3654 (1982)
16. T.J. Lee, A.P. Rendell, P.R. Taylor, J. Chem. Phys. **93**, 6636 (1990)
17. C.W. Bauschlicher Jr, H. Partridge, Chem. Phys. Lett. **300**, 364 (1999)
18. W. Klopper, L. Almlof, J. Chem. Phys. **99**, 5167 (1993)
19. F. Reuse, S.N. Khanna, V. de Coulon, J. Buttet, Phys. Rev. B **39**, 12911 (1989); *ibid.* **41**, 11743 (1990)
20. V. Kumar, R. Car, Phys. Rev. B **44**, 8243 (1991)
21. P. Delaly, P. Ballone, J. Buttet, Phys. Rev. B **45**, 3838 (1992)
22. U. Rothlisberger, W. Andreoni, P. Giannozzi, J. Chem. Phys. **96**, 1248 (1992)
23. X.G. Gong, Q.Q. Zheng, Y.Z. He, Phys. Lett. A **181**, 459 (1993)
24. L.A. Eriksson, J. Chem. Phys. **103**, 1050 (1995)
25. E.R. Davidson, R.F. Frey, J. Chem. Phys. **106**, 2331 (1997)
26. S.M. Riemann, M. Koskinen, H. Hakkinen, P.E. Lindelof, M. Manninen, Phys. Rev. B **56**, 12147 (1997)
27. A. Köhn, F. Weigend, R. Ahlrichs, Phys. Chem. Chem. Phys. **3**, 711 (2001)
28. J. Akola, K. Rytkonen, M. Manninen, Eur. Phys. J. D **16**, 21 (2001)
29. J. Akola, M. Manninen, H. Häkkinen, U. Landman, X. Li, L.-S. Wang, Phys. Rev. B **62**, 13216 (2000)